

This article was downloaded by:

On: 25 January 2011

Access details: *Access Details: Free Access*

Publisher *Taylor & Francis*

Informa Ltd Registered in England and Wales Registered Number: 1072954 Registered office: Mortimer House, 37-41 Mortimer Street, London W1T 3JH, UK



## Liquid Crystals

Publication details, including instructions for authors and subscription information:

<http://www.informaworld.com/smpp/title~content=t713926090>

### The SmA phase of a bent-core V-shaped compound: structure and electric-field response

Ibon Alonso<sup>a</sup>; Josu Martinez-Perdiguero<sup>a</sup>; Josu Ortega<sup>b</sup>; César Luis Folcia<sup>c</sup>; Jesús Etxebarria<sup>c</sup>; Nélida Gimeno<sup>d</sup>; María Blanca Ros<sup>d</sup>

<sup>a</sup> Micro and Nanotechnology Department, Fundación Tekniker, Eibar, Spain <sup>b</sup> Departamento de Física de la Materia Condensada, Facultad de Ciencia y Tecnología, Universidad del País Vasco, Bilbao, Spain

<sup>c</sup> Departamento de Física Aplicada II, Facultad de Ciencia y Tecnología, Universidad del País Vasco, Bilbao, Spain <sup>d</sup> Instituto de Ciencia de Materiales de Aragón, Química Orgánica, Facultad de Ciencias, Universidad de Zaragoza-CSIC, Zaragoza, Spain

Online publication date: 15 November 2010

**To cite this Article** Alonso, Ibon , Martinez-Perdiguero, Josu , Ortega, Josu , Folcia, César Luis , Etxebarria, Jesús , Gimeno, Nélida and Ros, María Blanca(2010) 'The SmA phase of a bent-core V-shaped compound: structure and electric-field response', *Liquid Crystals*, 37: 11, 1465 – 1470

**To link to this Article:** DOI: 10.1080/02678292.2010.521858

**URL:** <http://dx.doi.org/10.1080/02678292.2010.521858>

## PLEASE SCROLL DOWN FOR ARTICLE

Full terms and conditions of use: <http://www.informaworld.com/terms-and-conditions-of-access.pdf>

This article may be used for research, teaching and private study purposes. Any substantial or systematic reproduction, re-distribution, re-selling, loan or sub-licensing, systematic supply or distribution in any form to anyone is expressly forbidden.

The publisher does not give any warranty express or implied or make any representation that the contents will be complete or accurate or up to date. The accuracy of any instructions, formulae and drug doses should be independently verified with primary sources. The publisher shall not be liable for any loss, actions, claims, proceedings, demand or costs or damages whatsoever or howsoever caused arising directly or indirectly in connection with or arising out of the use of this material.

## The SmA phase of a bent-core V-shaped compound: structure and electric-field response

Ibon Alonso<sup>a</sup>, Josu Martinez-Perdiguero<sup>a</sup>, Josu Ortega<sup>b\*</sup>, César Luis Folcia<sup>c</sup>, Jesús Etxebarria<sup>c</sup>, Nélida Gimeno<sup>d</sup> and María Blanca Ros<sup>d</sup>

<sup>a</sup>Micro and Nanotechnology Department, Fundación Tekniker, Eibar, Spain; <sup>b</sup>Departamento de Física de la Materia Condensada, Facultad de Ciencia y Tecnología, Universidad del País Vasco, Bilbao, Spain; <sup>c</sup>Departamento de Física Aplicada II, Facultad de Ciencia y Tecnología, Universidad del País Vasco, Bilbao, Spain; <sup>d</sup>Instituto de Ciencia de Materiales de Aragón, Química Orgánica, Facultad de Ciencias, Universidad de Zaragoza-CSIC, Zaragoza, Spain

(Received 29 March 2010; final version received 3 September 2010)

The smectic A (SmA) phase of a V-shaped mesogen with a molecular bending angle of 60° was studied. According to X-ray measurements, the molecules are arranged with the ‘bow-string’ direction parallel to the smectic layer. This point was confirmed by birefringence analysis and the result is compatible with a non-polar structure. A detailed study of the (001) smectic layer reflection versus temperature was also carried out to determine the smectic translational order parameter. The results indicate that the material presents a high degree of translational order. In addition, the electric field response of the material was studied by means of second harmonic generation. This technique turned out to be highly sensitive to small structural distortions due to the V-shape of the constituent molecules.

**Keywords:** V-shaped molecule; second harmonic generation; X-ray; phase transition

### 1. Introduction

Among the different approaches to the synthesis of molecules to obtain liquid crystalline phases, bent-core compounds represent an outstanding family that has attracted the attention of the research community over the last years [1–3]. Some of the main reasons are the great variety of new phases and the interesting physical properties they present such as ferroelectricity, chirality or nonlinear optical properties.

However, the mesomorphism that bent-core compounds exhibit is very sensitive to chemical and morphological change, and therefore determination of the structure–activity links is not trivial. In this sense, one important molecular feature is the bending angle of the molecules and, depending on its value, bent-core compounds are usually classified in two families: banana compounds, when the bending angle is  $\alpha \sim 120^\circ$  and V-shaped for  $\alpha \sim 60^\circ$ . Typically, banana compounds form a great diversity of new mesophases different from the classical calamitic liquid crystalline phases [1–3]. On the contrary, V-shaped molecules, which have not been studied so extensively, present in most cases classical calamitic mesophases. However, this feature does not always hold, which makes it necessary to characterise the structural properties of the mesophases for every different compound. In addition, even when there are classical calamitic phases, the peculiar disposition of the molecular wings in the V-shaped compounds gives rise to different molecular arrangements inside the layers.

Several studies of the mesomorphism of this kind of materials can be found in the literature. For example the phase sequence nematic–SmA is often found [4–6]. In smectic A (SmA) phases, molecules can stack with their ‘bow-string’ parallel [7] or perpendicular to the smectic layers [4]. Apart from the classical SmA phase, there exists also the polar variant, which is more often found in banana compounds [7, 8]. In other cases the V-shaped compounds can exhibit bilayer smectic phases [4, 5], and even B4 phases [8, 9] usually found in banana compounds.

In this work we present an exhaustive study of the structural properties of the phases of one V-shaped compound whose synthesis and a preliminary characterisation study have been published previously [10]. In particular we have obtained some results on the molecular packing it presents in the SmA and crystalline phases. Additionally we have carried out studies of the smectic order parameter in the SmA phase by means of X-ray scattering experiments. Details of the experimental techniques used are described in the next section, followed by the presentation and discussion of the experimental results. Finally some conclusions are drawn.

### 2. Experimental

For texture observations and second harmonic generation (SHG) experiments, commercially available Linkam cells of 5  $\mu\text{m}$  thickness were used.

\*Corresponding author. Email: Josu.ortega@ehu.es

Birefringence measurements were performed using a Berek compensator in a polarised optical microscope (POM), Olympus BX-51. X-ray scattering measurements were carried out in Debye-Scherrer mode using powder samples confined in Lindemann capillaries of diameter 0.5 mm. A linear position-sensitive detector, with an angular resolution better than  $0.01^\circ$ , was employed to detect the diffracted intensity in the  $2\theta$  interval  $0.5\text{--}35^\circ$  ( $\theta$  is the diffraction angle). Monochromatic Cu-K $\alpha$ 1 radiation ( $\lambda = 1.5406 \text{ \AA}$ ) was used. SHG measurements were performed with an experimental set-up described in detail elsewhere [11]. The fundamental light is a Q-switched Nd-YAG laser (wavelength 1064 nm) with a pulse width of 6 ns and a frequency of 5 Hz. A square-wave electric field synchronised with the laser pulse was applied to the sample.

### 3. Results and discussion

The molecular structure and phase sequence of the studied compound is shown in Figure 1(a). The phase identification was carried out on the basis of differential scanning calorimetry (DSC) and texture observation by using POM.

Below the clearing point, a well-aligned nematic phase is obtained. On further cooling, a reasonably well-aligned SmA phase appears as can be seen in Figure 2. Under an electric field, no switching is observed when applying fields up to the damage threshold ( $25 \text{ V}/\mu\text{m}$ ). Some samples could resist fields as large as  $30 \text{ V}/\mu\text{m}$  [10]. At these high fields, the texture darkens indicating a tendency toward homeotropic orientation. However, these results were not reproducible. All the behaviours suggest that the mesophase is non-polar.

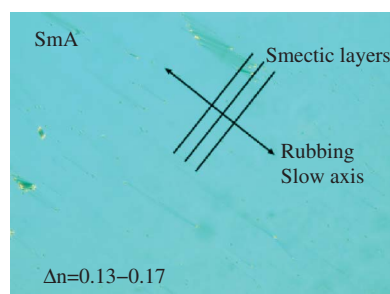


Figure 2. Optical texture of the studied compound in the SmA phase at  $155^\circ\text{C}$ . The rubbing direction and the smectic layers are sketched in the figure (colour version online).

As mentioned previously, the V-shape of the molecule gives rise to two possible inlayer molecular arrangements, i.e. with their 'bow-string' normal or parallel to the smectic layers (see Figure 1(b)). In order to clarify this point, small-angle X-ray scattering (SAXS) measurements were carried out. In the SmA phase, a single peak is observed corresponding to a periodicity of  $37 \text{ \AA}$  (see Figure 3). This distance is compatible with the molecular length along the 'bow-arrow' direction obtained in the most stable conformation. The calculation was performed using MM2 energy minimisation. This result and the absence of an electric field response point to a molecular arrangement as proposed in Figure 4(a).

Furthermore, we measured the birefringence in the sample from Figure 2. The obtained values in the whole temperature range of the phase were  $\Delta n = 0.13\text{--}0.17$ . It was also checked that, as expected, the slow axis of the indicatrix is parallel to the rubbing direction. The measured birefringence value is compatible with a model that considers the molecule as composed of two uniaxial wings with extraordinary and ordinary refractive indices  $n_e = 1.75$  and  $n_o = 1.5$ , respectively,

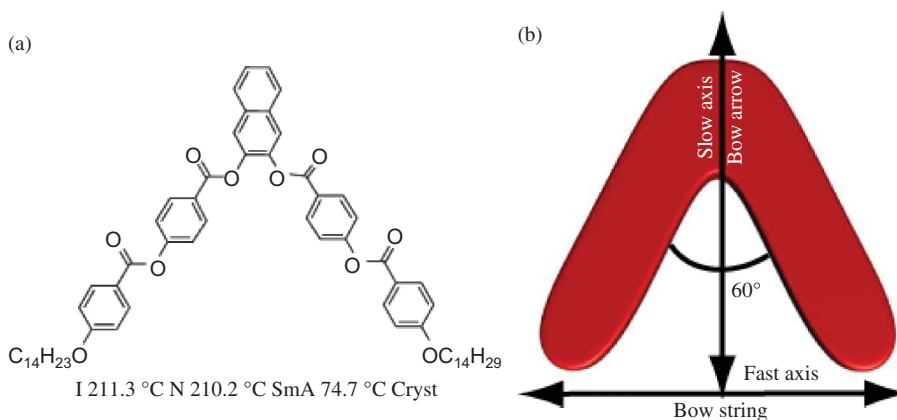


Figure 1. (a) Chemical structure and phase sequence of the studied compound. (b) Schematic representation of the V-shaped molecule. The most representative distances and the optical indicatrix axes are indicated.

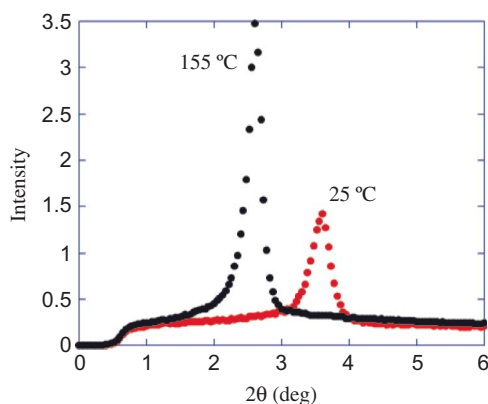


Figure 3. X-ray diffraction intensity versus scattering angle of the SmA (black points) and crystalline (red points) phases. The periodicities corresponding to both maxima are compatible with the ‘bow-string’ and ‘bow-arrow’ distances, respectively.

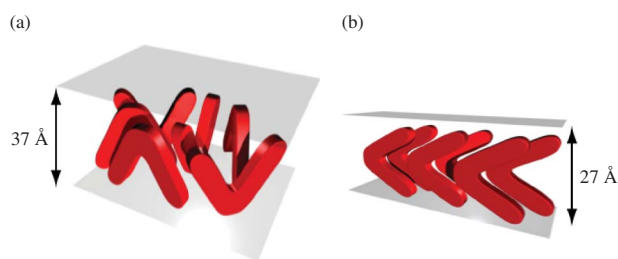


Figure 4. Inlayer molecular arrangement for (a) the SmA phase and (b) the lower temperature crystalline phase. The smectic layer spacing has been obtained from X-ray scattering measurements and is compatible with the molecular length in the sketched stacking.

making an angle of  $60^\circ$ . In fact, after averaging, the dielectric tensor under rotations along the normal to the smectic layer,  $\Delta n = 0.16$ , is obtained. Under this model, the slow axis corresponds to the direction of the arrow of the molecule and therefore the smectic layers are perpendicular to the rubbing direction.

On further cooling, the material undergoes a phase transition at  $74.7^\circ\text{C}$  and, in Linkam cells, the alignment is lost. The texture presents a reddish colour with circular domains (see Figure 5). In order to characterise this phase, X-ray scattering experiments were carried out in a wider angular range ( $2\theta$  interval  $0.5\text{--}35^\circ$ ). The diffraction diagram presents a sharp peak corresponding to a periodicity length of  $26.6 \text{ \AA}$  (red points in Figure 3), which indicates a lamellar structure of the phase. This distance is compatible with the length of the ‘bow-string’ of the molecule. At wider angles no diffuse halo appears. Instead a set of small peaks is observed. This fact implies an inlayer crystalline or hexatic order, which is consistent with the null response of the phase to electric fields.

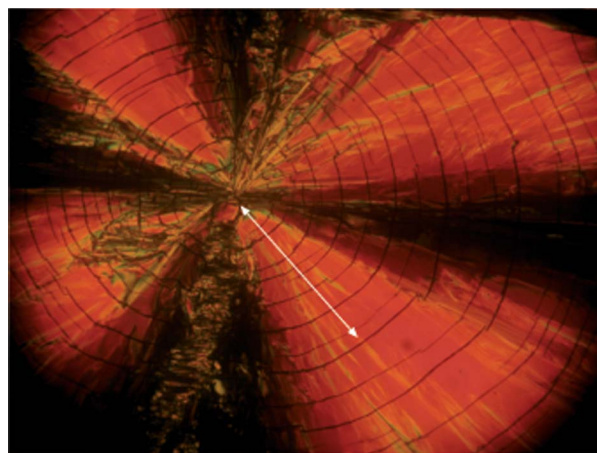


Figure 5. Optical texture of the crystalline phase at  $25^\circ\text{C}$ . The fast axis of the optical indicatrix was determined using a Berek compensator.

From an optical point of view, the texture depicted in Figure 5 presents a birefringence  $\Delta n = 0.23$ . The important increase in the birefringence suggests a biaxial structure, which is consistent with the optical model of the molecule previously considered provided a higher density and a higher molecular order is assumed in the crystalline phase. In this case, it is observed that the axis perpendicular to the layers corresponds to the fast axis. This implies that the molecules inside the layers are oriented with the ‘bow-string’ perpendicular to the layers. Figure 4(b) shows a possible molecular arrangement, but it is not possible to determine the precise dipolar moment disposition inside the layer.

In order to extract further information about the inlayer dipole arrangement, SHG measurements were carried out in both the SmA and the lower temperature crystalline phases. Measurements were made in homogeneously aligned cells at an incidence angle  $\phi_i = 30^\circ$ . The electric field was perpendicular to the glass substrates. The fundamental light was polarised linearly along the rubbing direction and the analyser was set parallel to the polariser. Measurements were carried out in the SmA phase at  $190^\circ\text{C}$  and the crystalline phase at  $60^\circ\text{C}$ .

In the SmA phase, no SHG signal is detected without a field. This is in agreement with the structure proposed in Figure 4(a) since it is centrosymmetric and therefore SHG is forbidden. Under an electric field, however, an SHG signal is observed. Figure 6(a) shows the SHG intensity versus electric field. Assuming phase matching configuration, the SHG power is given by the expression:

$$P(2\omega) = AL^2 d_{\text{eff}}^2 P(\omega)^2, \quad (1)$$



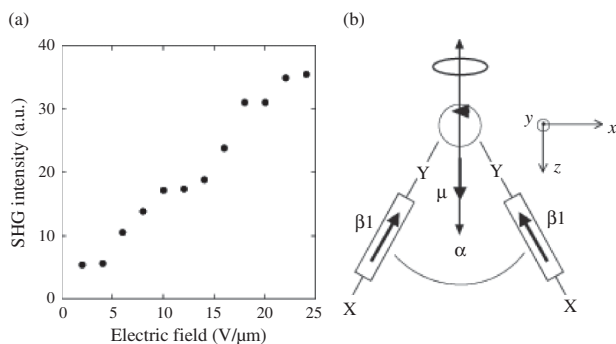


Figure 6. (a) SHG intensity of the SmA phase versus electric field. Measurements were carried out at 190°C. (b) Scheme of nonlinear response of the V-shaped molecule. The hyperpolarisability is mainly driven by the longitudinal component  $\beta_1$ . The dipolar moment  $\mu$  is also depicted in the figure.

where  $L$  is the sample thickness,  $P(\omega)$  is the power of the fundamental light,  $A$  is a constant that depends mainly on the geometry of the experimental set-up and  $d_{eff}$  is a parameter that is related to the second-order susceptibility coefficients involved in the experimental configuration of the sample and light polarisation.

Comparing the SHG signal with that of a y-cut quartz crystal ( $d_{11} = 0.4$  pm/V), the unknown parameters of Equation (1) can be deduced, and for an electric field of  $24\text{V}/\mu\text{m}$ , we obtained  $d_{eff} = 0.02$  pm/V. This result is surprising since, as previously mentioned, no changes were observed in the texture of the material when applying electric fields up to the damage threshold.

In order to explain the SHG behaviour we will use the microscopic approach proposed by Araoka *et al.* [12] for the nonlinear optical response of the molecule. Under this model, the main contribution to the SHG response is due to the longitudinal hyperpolarisability along the molecular wings ( $\beta_l$ ) as shown in Figure 6(b), and the whole molecule presents two independent hyperpolarisability tensor components in the  $xyz$  frame given by

$$\begin{aligned}\beta_{zzz} &= 2 \cos^3\left(\frac{\alpha}{2}\right)\beta_l \\ \beta_{zxx} &= 2 \cos\left(\frac{\alpha}{2}\right) \sin^2\left(\frac{\alpha}{2}\right)\beta_l.\end{aligned}\quad (2)$$

As previously commented, the second-order susceptibility tensor  $\mathbf{d}$  of the SmA phase under no field is null as the phase is centrosymmetric (Figure 7(a)). However, the field induces a distortion on the structure, as sketched in Figure 7(b), and in this case SHG symmetry is allowed.

The  $\mathbf{d}$  tensor associated to the distorted structure can be obtained as follows. First we calculate

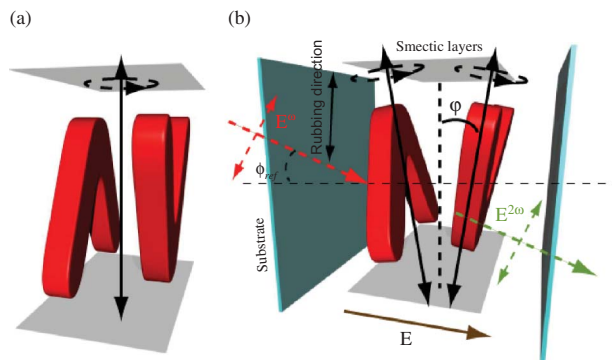


Figure 7. Scheme of the electric field induced distortion in the SmA phase. (a) Inlayer molecular stacking under no field. The actual structure presents rotational symmetry along the normal to the smectic layers as indicated in the figure by the dashed circle. (b) Induced distortion by the electric field. The molecule on the left together with the dashed circle schematises a set of molecules corresponding to  $\mathbf{d}_{up}$  with rotational symmetry (SmA symmetry) and tilted by an angle  $\varphi$ . The molecule on the right represents the analogous situation for the case  $\mathbf{d}_{down}$ . The  $\mathbf{d}$  tensor of the whole structure is the average of  $\mathbf{d}_{up}$  and  $\mathbf{d}_{down}$ . The experimental configuration of the SHG experiment is also indicated (colour version online).

the contribution of the molecules under no field with the ‘bow-arrow’ pointing up separately from those pointing down. To calculate these tensors, we take the contribution from a single molecule (e.g. dipole moment up) and average the tensor due to the rotational symmetry of the SmA phase along the normal to the smectic layer. The tensor obtained, named  $\mathbf{d}_{up}$ , accounts then only for the molecules with ‘bow-arrow’ pointing up. Thus, the equation in contracted notation in a frame system with  $Z$  perpendicular and  $X, Y$  parallel to the smectic layers is

$$\mathbf{d}_{up} = \begin{pmatrix} 0 & 0 & 0 & 0 & D/2 & 0 \\ 0 & 0 & 0 & D/2 & 0 & 0 \\ D/2 & D/2 & d & 0 & 0 & 0 \end{pmatrix}, \quad (3)$$

where  $D = Nf^3\beta_{zxx}$  and  $d = Nf^3\beta_{zzz}$ ,  $N$  is the density of molecules and  $f$  is a local field factor. The contribution of the molecules with the arrow pointing down is  $\mathbf{d}_{down} = -\mathbf{d}_{up}$  as these tensors are related by  $\pi$  rotation along  $X$  (or  $Y$ ) and, therefore, it is evident that the head–tail invariance of the SmA mesophase averages the  $\mathbf{d}$  tensor of the non distorted structure out to zero. However, the  $\mathbf{d}$  tensor of the distorted structure can now be calculated simply by rotating the tensor of Equation (3) by an angle  $\varphi$  along the direction parallel to the smectic layer and perpendicular to the electric field (see Figure 7(b)), and subsequently applying the head–tail invariance, i.e. averaging it with the contribution of the equivalent structure of the molecules with

the ‘bow-arrow’ pointing down. In our SHG experimental configuration (see Figure 7(b)),  $d_{eff}$  is given approximately by the equation

$$d_{eff} = 3(D - d) \cos^2(\phi_{ref}) \sin(\phi_{ref}) \cos^2(\varphi) \sin(\varphi), \quad (4)$$

where  $\phi_{ref}$  is the refraction angle of the fundamental light when entering the sample and  $\varphi$  is the distortion angle of the molecules due to the electric field. For a value of  $(D - d) \sim 1$  pm/V (typical in banana compounds [13]), the measured SHG efficiency can be accounted for by a distortion angle  $\varphi \sim 1^\circ$ . It is impossible to perceive this small perturbation perceived by direct texture observation, but it is detectable by SHG measurements due to the high sensitivity of this technique to small perturbations in the structure of bent-core mesophases.

In the crystalline phase, SHG response was detected without an electric field. This result proves the biaxiality of the phase suggested by the optical studies since the result implies a ferroelectric molecular arrangement inside the layers. A scheme of the inlayer molecular disposition is shown in Figure 4(b). It is worth mentioning that the SHG behaviour of this compound resembles that found by Weissflog *et al.* [14] for a four-ring bent-core material presenting a calamitic SmA phase and a low-temperature crystal phase. SHG is induced by applying an electric field in the SmA phase, whereas a nonlinear signal is observed without field in the crystalline phase.

Finally a study of the order parameter in the SmA phase was carried out by means of X-ray scattering studies. In particular, the integrated intensity of the (001) peak as a function of the temperature was measured near the N–SmA transition following the procedure explained by Kapernaum and Giesselmann [15]. The smectic translational order parameter  $\Sigma$  is defined as the average amplitude of the density wave and is given by the equation

$$\Sigma = \left\langle \cos\left(\frac{2\pi z_i}{d}\right) \right\rangle, \quad (4)$$

where  $d$  is the layer spacing and  $z_i$  the position of the molecule  $i$  measured from an origin that makes the order parameter maximum.  $\Sigma$  can be obtained by comparing the (001) peak intensity  $I$  measured at a given temperature with the same peak but assuming a perfect translational order ( $I_o$ ). The relation is given by [16]

$$\Sigma^2 = \frac{I(T)}{I_o}. \quad (5)$$

$I_o$  can be obtained by extrapolation of the  $I(T)$  function to  $T = 0$ , since at this temperature, the hypothetical smectic structure is expected to be perfectly ordered. Following the general theory of phase transitions, the smectic order parameter can be expressed in terms of the reduced temperature as follows:

$$\Sigma = |\tau|^\beta, \quad (6)$$

where  $\tau = (T/T_C) - 1$ ,  $T_C$  is the phase transition temperature from the nematic to SmA phases and  $\beta$  is the critical exponent of the transition. Combining Equations (5) and (6), it is straightforward to obtain

$$I(T) = I_o [(T/T_C) - 1]^{2\beta}. \quad (7)$$

The parameters  $I_o$  and  $\beta$  can be calculated by fitting the integrated intensities of the (001) peak versus temperature. Figure 8 shows  $I(T)$  at the SmA phase and the best fit (red line,  $I_o = 290$ ,  $\beta = 0.06$ ), together with the line corresponding to perfect smectic order ( $\beta = 0$ ,  $\Sigma = 1$ , black line). According to the quality of the fit, the order parameter well inside the SmA phase can be considered to be in the range  $0.9 < \Sigma < 1$ , which implies highly ordered smectic layers compared with other calamitic SmA phases as reported by Kapernaum and Giesselmann [15]. Since it presents a degree of smectic order comparable to our compound, it is worth making a comment concerning the compound 3M 8422 studied in that work [15], which presents a ‘de Vries’ type SmA phase. In this respect it is important to remark on the similarity of both phases if we consider the molecular wings of our V-shaped

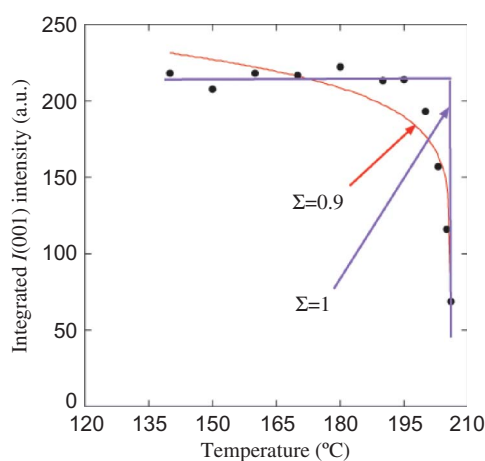


Figure 8. Integrated intensity of the (001) peak as a function of the temperature in the SmA phase. The blue line corresponds to the case of perfect smectic order ( $\beta = 0$  in Equation (7)). The red line corresponds to the best-fit,  $\beta = 0.06$  and  $I_o = 290$ , which implies that  $\Sigma = 0.9$  well inside the SmA phase (colour version online).

compound as calamitic molecules. A possible explanation for the high smectic order could be that the azimuthal wing distribution inside the layer is expected to suppress out-of-layer fluctuations.

#### 4. Concluding remarks

In this work several experimental techniques were used to determine the structural properties of the SmA phase of a V-shaped compound. The molecules were found to be stacked with the 'bow-arrow' parallel to the smectic layer forming a non-polar phase. In addition, the response of the material to electric fields was studied using SHG measurements. This technique turns out to be a very sensitive tool for detecting small distortions in bent-core compounds that are difficult to observe using other experimental procedures. In addition, a study of the smectic order parameter based on X-ray scattering measurements was performed for the first time in a V-shaped compound. The conclusion drawn is that the phase is highly ordered compared with other calamitic SmA phases and is comparable to a reported example of a 'de Vries' type mesophase. This is an interesting conclusion and can be explained in terms of certain similarities between both phases.

Finally the lower temperature crystalline phase was studied. The structure is lamellar and highly polar since SHG signal is found without an electric field. Surprisingly, the inlayer molecular arrangement implies a 90° rotation of the molecules with respect to the smectic layers and therefore the transition from the SmA phase implies a deep structural change.

#### Acknowledgements

This research was supported by CICYT-FEDER of Spain-UE MAT2008-06522-CO2 and MAT2009-14636-CO3, the

Aragón Government (E04), and the Basque Country Government (Project No. GIC-10/45). N.G. acknowledges the Spanish Government for a Juan de la Cierva fellowship.

#### References

- [1] Pelzl, G.; Diele, S.; Weissflog, W. *Adv. Mater.* **1999**, *11*, 707–724.
- [2] Amaranatha Reddy, R.; Tschierske, C. *J. Mater. Chem.* **2006**, *16*, 907–961.
- [3] Takezoe, H.; Takanishi, Y. *Jpn. J. Appl. Phys.* **2006**, *45*, 597–625.
- [4] Attard, G.S.; Douglass, A.G. *Liq. Cryst.* **1997**, *22*, 349–358.
- [5] Yelamaggad, C.V.; Shashikala, I.; Shankar Rao, D.S.; Krishna Prasad, S. *Liq. Cryst.* **2004**, *31*, 1027–1036.
- [6] Prasad, V. *Liq. Cryst.* **2001**, *28*, 145–150.
- [7] Lee, S.K.; Shi, L.; Ishige, R.; Kang, S.; Tokita, M.; Watanabe, J. *Chem. Lett.* **2008**, *37*, 1230–1231.
- [8] Lee, S.K.; Li, X.; Kang, S.; Tokita, M.; Watanabe, J. *J. Mater. Chem.* **2009**, *19*, 4517–4522.
- [9] Lee, S.K.; Naito, Y.; Shi, Lu.; Tokita, M.; Takezoe, H.; Watanabe, J. *Liq. Cryst.* **2007**, *34*, 935–943.
- [10] Gimeno, N.; Clemente, M.J.; Forcén, P.; Serrano, J.L.; Ros, M.B. *New J. Chem.* **2009**, *33*, 2007–2014.
- [11] Pereda, N.; Folcia, C.L.; Etzebarria, J.; Ortega, J.; Ros, M.B. *Liq. Cryst.* **1998**, *24*, 451–456.
- [12] Araoka, F.; Park, B.; Kinoshita, Y.; Ishikawa, K.; Takezoe, H.; Thisayukta, J.; Watanabe, J. *Jpn. J. Appl. Phys.* **1999**, *38*, 3526–3529.
- [13] Pintre, I.C.; Gimeno, N.; Serrano, J.L.; Ros, M.B.; Alonso, I.; Folcia, C.L.; Ortega, J.; Etzebarria, J. *J. Mater. Chem.* **2007**, *17*, 2219–2227.
- [14] Weissflog, W.; Dunemann, U.; Findelsen-Tandel, S.; Tamba, M.G.; Kresse, H.; Pelzl, G.; Diele, S.; Baumeister, U.; Eremin, A.; Stern, S.; Stannarius, R. *Soft Matter* **2009**, *5*, 1840–1847.
- [15] Kapernaum, N.; Giesselmann, F. *Phys. Rev. E: Stat., NON linear, Soft Matter Phys.* **2008**, *78*, 062701–1–3.
- [16] Leadbetter, A.J. In *The Molecular Physics of Liquid Crystals*; Luckhurst, G., Gray, G., Eds.; Academic Press: London, 1979.